Parametrically Excited Nonlinear Two-Degree-of-Freedom Electromechanical Systems

IOP Conf. Series: Journal of Physics: Conf. Series **1264** (2019) 012024 doi:10.1088/1742-6596/1264/1/012024

Parametrically Excited Nonlinear Two-Degree-of-Freedom Electromechanical Systems

Bahareh Zaghari [1], Till Kniffka [2], Cameron Levett [3], and Emiliano Rustighi [3]

[1] Electronics and Computer Science (ECS), University of Southampton, Southampton, SO17 1BJ, UK
[2] Institute of Mechanics and Mechatronics, TU Wien, Getreidemarkt 9, 1060 Vienna, AT
[3] Institute of Sound and Vibration (ISVR), University of Southampton, Southampton, SO17 1BJ, UK

E-mail: bahareh.zaghari@soton.ac.uk

Abstract. This paper presents a nonlinear parametrically excited cantilever beam with electromagnets. A parametrically excited two-degree-of-freedom (2-DOF) system with linear time-varying stiffness, nonlinear cubic stiffness, nonlinear cubic parametric stiffness and nonlinear damping is considered. In previous studies the stability and bifurcation of the nonlinear parametrically excited 2-DOF were investigated through analytical, semi-analytical and numerical methods. Unlike previous studies, in this contribution the system's response amplitude and phase at parametric resonance and parametric combination resonance are demonstrated experimentally and some novel results are discussed. Experimental and analytical amplitude-frequency plots are presented to show the stable solutions. Solutions for the system response are presented for specific values of parametric excitation frequency and the energy transfer between modes of vibrations is observed. The results presented in this paper prove that the bifurcation point and hence the bandwidth of the parametric resonance can be predicted correctly with the proposed analytical method. The proposed nonlinear parametrically excited 2-DOF can be used to design Micro ElectroMechanical Systems (MEMS) actuators and sensors. Validating the experimental results with the theory can improve the efficiency of these electrical systems.

1. Introduction

The majority of research on parametric excitation (PE) addresses systems with undesirable excitations. Typical examples for technical systems which suffer from PE are pantographs [1], wind-turbines [2] and asymmetric rotors [3]. However, PE can be exploited for energy harvesting [4]. Parametric excitation at anti-resonance can be exploited to reduce vibration. Dohnal [5] presented the stability of a linear multi degree of freedom system and vibration suppression by employing variable-stiffness. PE vibrations often require attention, since they differ significantly from externally excited (forced) vibrations. While the amplitudes of vibrations increase linearly over time at an ordinary resonance, they increase exponentially over time at a so-called parametric resonance (PR). This is due to an instability of a system's rest position caused by PE. Second, the vibrations' amplitudes at PRs are only limited by non-linearities which in most technical systems are small. Thus vibration amplitudes generally are much larger

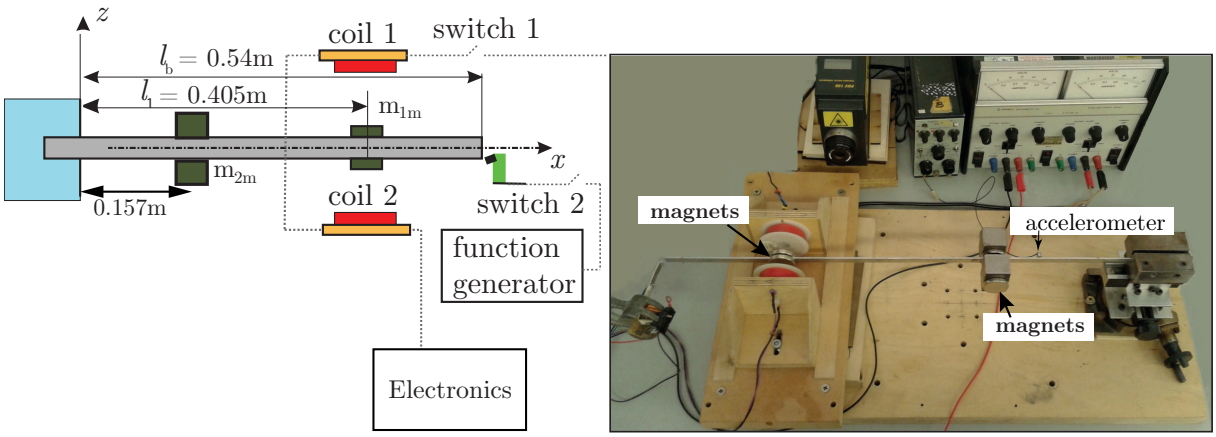

Figure 1: Experimental set-up consisting of a cantilever beam and an electromagnetic system.

at PRs than in ordinary resonance cases. Third, PRs are very narrow compared to ordinary resonances, but even low degree of freedom systems may experience multiple PRs.

The increasing computational power available and improvements in user friendly simulation software have led to a better understanding, and hence to a growing number of systems actively using PRs. However, for MDOF systems little progress has been made regarding both analytical and numerical methods for investigation. Partly this is caused by the problem of choosing a meaningful reduction of the systems phase space to investigate and display the results. The quasi-modal reduction of the phase space presented in [6] solves this problem by reducing MDOF models to one degree of freedom (1-DOF) models at PR. This enables the investigation of non-linear MDOF PE systems analytically, and to display the results of analytical and numerical investigations.

While recently advances have been made explaining and describing the behaviour of PE systems at PR analytically and numerically (e.g. [7]), these investigations lack validation with physical experiments. This paper presents analytical and experimental results for a 2-DOF nonlinear PE system together.

2. Modelling

A clamped-free cantilever beam with an electromagnetic system and two masses is shown in Figure 1. A controllable current is generated and flows through the coils to generate time-varying and nonlinear stiffness and damping [8]. The electromagnetic set-up was modified based on the work of Dohnal [9]. The modified test rig was used to exploit parametric excitation for vibration energy harvesting [4]. For the study presented in this paper the extra mass is added to change the ratio between the first and the second resonance. The mechanical properties, dimensions of the cantilever beam, and the electromagnetic system are shown in Table 1. A Two Degree of Freedom (2-DOF) model of this NPE system is presented in Figure 2. In Figure 2, k_{02} and k_{12} are the linear stiffnessess. k_{01} has linear and nonlinear stiffness components,

$$k_{01} = k_{01,\mathrm{lin}} + k_{01,\mathrm{nlin}} {x_1}^2, \tag{1}$$

and the time-varying and nonlinear stiffness is

$$k_1 = k_{\mathrm{PE},1,\mathrm{lin}} + k_{\mathrm{PE},1,\mathrm{nlin}} {x_1}^2. \tag{2}$$

The equation of motion for the model shown in Figure 2 is

$$\mathbf{M}\ddot{\mathbf{x}} + \mathbf{C}\dot{\mathbf{x}} + \mathbf{K}_{\mathrm{lin}}\mathbf{x} + \mathbf{K}_{\mathrm{PE},1,\mathrm{lin}} \cos(\Omega_{\mathrm{PE}} t)\mathbf{x} + \mathbf{K}_{\mathrm{nlin}}\mathbf{x}^3 + \mathbf{K}_{\mathrm{PE},1,\mathrm{nlin}} \cos(\Omega_{\mathrm{PE}} t)\mathbf{x}^3 = \mathbf{0}, \tag{3}$$

Table 1: Mechanical properties and dimensions.

Property	Values	Units
Radius of the magnets	0.015	m
Residual magnetic flux density (B_r)	1.1	T
Permeability (μ_0)	$4 \times \pi \times 10^{-7}$	$\mathrm{N\,A^{-2}}$
Inner radius of the coil (r_1)	0.0085	m
Outer radius of the coil (r_2)	0.0225	m
Mean radius of the coil (r_c)	0.0135	m
Number of turns of in coil (N)	485	-
Length of wire in one rotation (l_w)	0.078	m
Diameter of the coil (D_w)	0.00071	m
Height of the coil with shield (h_coil)	0.02	m
Coordinate for coil (z_1)	0.007	m
Coordinate for coil (z_2)	-0.007	m
Resistance of the coil (R_coil)	1.91	Ohm
Inductance of the coil (L_coil)	0.00064	$\mathrm{kg\,m^2\,s^2\,A^2}$
Load resistor (R)	0.1	Ohm
Width of the beam (b_b)	0.01	m
Thickness of the beam (t_b)	0.002	m
Measured mass 1 (m_1m)	0.07	kg
Measured mass 2 (m_2m)	0.658	kg
Half of the distance between the coils (h)	0.03	m
Measured first natural frequency of the beam with masses and $I_\mathrm{c} = 0$ ($\omega_\mathrm{n1,exp}$)	30.45	$\mathrm{rad\,s^{-1}}$
Measured second natural frequency of the beam with masses and $I_\mathrm{c} = 0$ ($\omega_\mathrm{n2,exp}$)	55.13	$\mathrm{rad\,s^{-1}}$

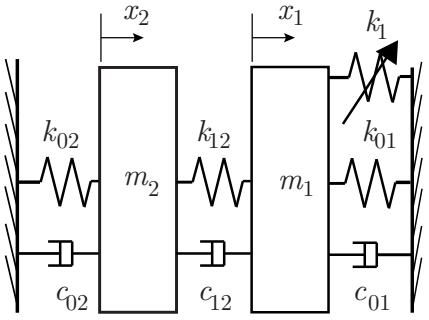

Figure 2: Mechanical two degree of freedom, lumped mass model of the experimental system in Figure 1.

where the overdot represents a derivative with respect to time t, and where the mass displacements are $\mathbf{x} = \begin{bmatrix} x_1 \\ x_2 \end{bmatrix}$. The mass matrix $\mathbf{M}$ is

$$\mathbf{M} = \begin{bmatrix} m_1 & 0 \\ 0 & m_2 \end{bmatrix}. \tag{4}$$

The damping matrix $\mathbf{C}$ is

$$\mathbf{C} = \begin{bmatrix} c_{01} + c_{12} & -c_{12} \\ -c_{12} & c_{12} + c_{02} \end{bmatrix}. \tag{5}$$

The stiffness matrix has linear, linear time-varying, and nonlinear components:

$$\mathbf{K}_{\text{lin}} = \begin{bmatrix} k_{01,\text{lin}} + k_{12} & -k_{12} \\ -k_{12} & k_{02} + k_{12} \end{bmatrix}, \tag{6}$$

$$\mathbf{K}_{\text{PE,1,lin}} = \begin{bmatrix} k_{\text{PE,1,lin}} & 0 \\ 0 & 0 \end{bmatrix}, \tag{7}$$

$$\mathbf{K}_{\text{nlin}} = \begin{bmatrix} k_{01,\text{nlin}} & 0 \\ 0 & 0 \end{bmatrix}, \tag{8}$$

$$\mathbf{K}_{\text{PE,1,nlin}} = \begin{bmatrix} k_{\text{PE,1,nlin}} & 0 \\ 0 & 0 \end{bmatrix}. \tag{9}$$

3. Model calibration

In order to find $k_{01,\text{lin}}$, k_{12}, k_{02}, m_1, and m_2 based on the experimental modal analysis, several impact tests were conducted. The first natural frequency 30.458rad s^{-1} and the second natural frequency 55.14rad s^{-1}, when I_{DC}=0A were flowing in the coils were measured. Similar tests were carried out when I_{DC}=1A were flowing in the coils, and the first natural frequency 31.77rad s^{-1} and the second natural frequency 58.46rad s^{-1} were measured. The impact tests were applied in a way that the beam displacement was small and hence the effect of nonlinear parameters were minimised and the coherence was reduced.

Eigenvalues for the first and the second mode was obtained from the experimental tests.

Given that the damping is assumed to be zero the eigenvalues are pure imaginary and the eigenvectors are real. The eigenvalue problem can be simplified to

$$(\mathbf{K}_{\text{lin}} - \omega^2 \mathbf{M})\Phi = \mathbf{0}. \tag{10}$$

ω can be found from $\det\left|\mathbf{K}_{\text{lin}} - \omega^2\mathbf{M}\right| = \mathbf{0}$,

$$\omega_{1,2} = \frac{(k_{02}+k_{12})m_1 + (k_{01,\text{lin}}+k_{12})m_2}{2m_1m_2} \pm \frac{\sqrt{\left((k_{02}+k_{12})^2m_1^2 + (k_{01,\text{lin}}+k_{12})^2m_2^2 - 2(k_{02}+k_{12})(k_{01,\text{lin}}+k_{12})m_1m_2 + 4(k_{12})^2m_1m_2\right)}}{2m_1m_2} \tag{11}$$

so the eigenvalues are:

$$\Phi = \left[\begin{pmatrix}\phi_1\\ \phi_2\end{pmatrix}_1 \begin{pmatrix}\phi_1\\ \phi_2\end{pmatrix}_2\right] \tag{12}$$

From Eq. (10)

$$\begin{bmatrix} (-m_1\omega^2 + k_{01,\text{lin}} + k_{12})\phi_1 - k_{12}\phi_2 \\ -k_{12}\phi_1 + (-m_2\omega^2 + k_{02} + k_{12})\phi_2 \end{bmatrix} = \mathbf{0} \tag{13}$$

We can say for the first resonance

$$\left(\frac{\phi_1}{\phi_2}\right)_1 = \frac{k_{12}}{-m_1\omega_1^2 + k_{01,\text{lin}} + k_{12}} = 6.6 \tag{14}$$

Table 2: System parameters

Parameters	Values	Units
m_1	0.2	kg
m_2	0.67	kg
$k_{12,\mathrm{lin}}$	40	Nm^{-1}
$k_{02,\mathrm{lin}}$	2200	Nm^{-1}
$k_{01,\mathrm{lin}}$	168.23	Nm^{-1}
$k_{\mathrm{PE},1,\mathrm{lin}}$	12.61	Nm^{-1}
$k_{01,\mathrm{nlin}}$	2.3×10^5	Nm^{-3}
$k_{\mathrm{PE},1,\mathrm{nlin}}$	1.8×10^4	Nm^{-3}

and for the second resonance

$$\left(\frac{\phi_1}{\phi_2}\right)_2 = \frac{-m_2\omega_2^2 + k_{02} + k_{12}}{k_{12}} = -0.08 \tag{15}$$

From Eqs. (14) and (15) and the analytical expression for linear stiffness due to electromagnets we can find the system parameters as stated in Table 2. $k_{01,\mathrm{lin}}$ and $k_{01,\mathrm{nlin}}$ are calculated analytically and they are function of coils parameters and DC current flowing in the coils, and $k_{01,\mathrm{lin}} = I_{\mathrm{DC}}H_1$ (H_1 refers to Eq. (16) in [8]). $k_{01,\mathrm{nlin}} = I_{\mathrm{DC}}H_2$ (H_2 refers to Eq. (17) in [8]).

$k_{\mathrm{PE},1,\mathrm{lin}}$ and $k_{\mathrm{PE},1,\mathrm{nlin}}$ are function of AC current, where $k_{\mathrm{PE},1,\mathrm{lin}} = I_{\mathrm{AC}}H_1$ and $k_{\mathrm{PE},1,\mathrm{nlin}} = I_{\mathrm{AC}}H_2$. These linear and nonlinear stiffness are calculated for I_{DC}=1A and I_{AC}=0.075A and the results are stated in Table 2.

The analytical solution presented in this paper is defined for a system with small damping. Here, damping is found based on the experimental tests. Damping ratios of the first and the second mode, $\zeta_1 = 0.000513$ and $\zeta_2 = 0.0003$, were measured from the impact tests with a circle-fit method. Hence, we considered the damping to be negligible.

4. Analytical study

The eigenvectors stated Eq. (14) and Eq. (15) can be mass normalised so that

$$\boldsymbol{\varphi}_i^{\mathrm{T}}\mathbf{M}\boldsymbol{\varphi}_i = \mathbf{1} \tag{16}$$

leads to $\boldsymbol{\varphi}_1 = [2.1552\ 0.3255]^{\mathrm{T}}$ and $\boldsymbol{\varphi}_2 = [0.1025\ -1.2204]^{\mathrm{T}}$. These mass normalised eigenvectors can be summarised in the modal matrix $\boldsymbol{\Phi} = [\boldsymbol{\varphi}_1\ \boldsymbol{\varphi}_2\ ...\ \boldsymbol{\varphi}_n]$. This matrix is employed for a transformation of the displacement vector $\mathbf{x}$ into the quasi-modal displacements $\mathbf{z}$ by

$$\mathbf{x} = x^*\boldsymbol{\Phi}\mathbf{z}. \tag{17}$$

The scaling parameter x^* is utilised in order to have dimensionless quasi-modal displacements $\mathbf{z}$. Here $x^* = 10^{-3}$ m is set, which enforces an appropriate scaling when evaluating the differential equations numerically. For a linear time-invariant system, $\mathbf{z}$ are the natural modes. Furthermore, this transformation decouples the differential equations for this linear, time-invariant system. However, Eq. (3) cannot be decoupled, because the transformation above couples the equations of motion by the terms due to the parametrical excitation. Nonetheless, for a PE system the quasi-modal displacements z_i represent the vibrations regarding each mode. Hence, the term *quasi-modal* is used [7]. The eigentime $\tau = \Omega_{\mathrm{PE}}t$ is also introduced to normalise time. Applying the above described quasi-modal transformation, Eq. (3) leads to

$$\mathbf{z}'' + \mathbf{Z}\mathbf{z}' + \boldsymbol{\Lambda}\mathbf{z} + \boldsymbol{\Lambda}_{\mathrm{nlin}}(\mathbf{z})\mathbf{z} + \mathbf{E}(\mathbf{z})\cos(\tau)\mathbf{z} = \mathbf{0}. \tag{18}$$

Table 3: Relevant quasi-modally reduced parameters.

Parameters	Values
κ_1^2	2.805
$\epsilon_{1,\text{lin}}$	127.8
$\epsilon_{1,\text{nlin}}$	0.387

Each line of this matrix equation states the vibration of one mode. At PR predominantly the mode i can be observed which agrees with the PR frequency $\Omega_{\text{PR},n} = \frac{2\omega_i}{n}$. Similarly, both modes i and j can be observed at Parametric Combination Resonances PCRs with the angular centre frequency $\Omega_{\text{PCR},n} = \frac{\omega_i+\omega_j}{n}$. The quadratic and bilinear terms in $\mathbf{\Lambda}_{\text{nlin}}(\mathbf{z})$ and $\mathbf{E}(\mathbf{z})$ can be set to zero except for terms containing z_i^2 because the dominant mode's amplitude is sufficiently larger than the one of all other modes. This reduces the multi-dimensional problem of Eq. (18) to a scalar one. Consequently, at a PR the vibrations of the n bodies of the MDOF system can be approximated by $x_k \approx x^* \varphi_{ik} z_i$ for the kth body where, i refers to the quasi-mode φ_i and φ_{ik} is its kth element. Averaging according to Krylov-Bogolyubov [10] over one period of $z_i(\tau)$ ultimately leads to

$$z_i \approx \bar{r}_i \cos(2\tau + \bar{\psi}_i),\ \bar{r}_i = \sqrt{\frac{8\pi\omega_i \Delta f + 2\epsilon_{i,\text{lin}}}{-2\epsilon_{i,\text{nlin}} + 3\kappa_i^2(1 - \frac{2\pi\Delta f}{\omega_i})}},\ \bar{\psi}_i = \frac{\pi}{2} \tag{19}$$

assuming the deviation of the PE frequency from the centre frequency of the PR to be very small (see [7] for a detailed explanation). This can be considered if the amplitude of the only stable bifurcation within the instability band of the rest position is at the ith first PR $f_{\text{PE}} = 2f_i$. Here $\Delta f = f - f_{\text{PE}}$ denotes the deviation from the PR centre frequency. For a 2-DOF system, κ_i^2 is the first (i.e. upper left) element of $\mathbf{\Lambda}_{\text{nlin}}$ in case of $i = 1$ and the last element (i.e. lower right) in case of $i = 2$. In analogy, $\epsilon_{i,\text{lin}}$ and $\epsilon_{i,\text{nlin}}$ are the first elements (in case of $i = 1$) or the last elements (in case of $i = 2$) of the linear part and the nonlinear part of $\mathbf{E}$. At the first PR for the parameters stated in Table 2 the relevant quasi-modaly reduces parameters take the values listed in Table 3. Note that by Eq. (19) the frequency of the bifurcated solution is predicted to be twice the PE frequency and the phase shift to be $\bar{\psi}_i = \frac{\pi}{2}$ which agrees with numerical studies.

5. Experimental results

Displacement of the first and the second mass was found from recorded velocity and acceleration at two points on the cantilever beam. The accelerometer and the vibrometer are shown in Figure 1. The accelerometer was placed at 0.105m from support end, and the vibrometer was measuring the beam velocity at 0.305m from support end. Due to the influence of magnets, the accelerometer was not placed close to the second mass. For future studies several vibrometers are needed to look at the vibration at different positions.

The displacement of the first mass $m_{1\text{m}}$ was found from the recorded vibration when the parametric frequency was increased for sweep up tests from 5Hz-20Hz. Sweep down tests were also carried out from high to low frequencies. In this experiment, the parametric frequency was increased or decreased in increments of 0.1Hz.

The tests were started with initial conditions of $z(0) = 0.01$m and as the steady-state response was achieved the tests were carried out with the previous state. The recorded vibrations is integrated to find the displacement for sweep up and down tests (Figure 3). The recorded displacement is multiplied by 1.43 to find the displacement of m_{1m}.

Displacement of the first mass $m_{1\text{m}}$ at different parametric frequencies are shown in Figure 4.

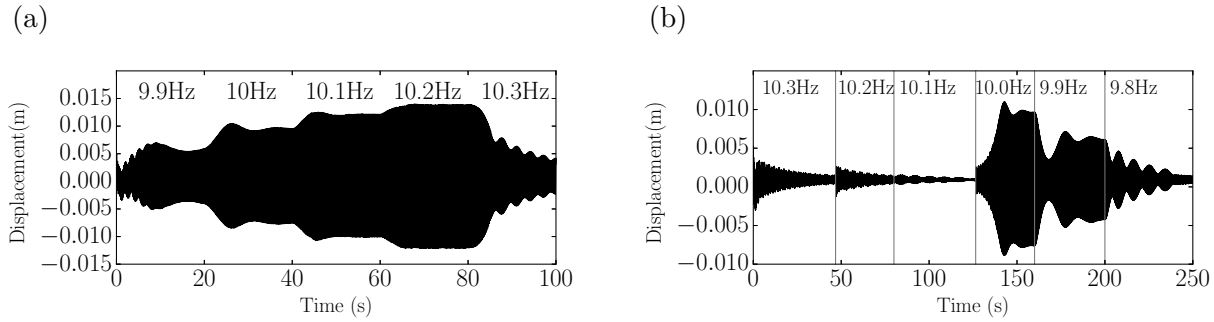

Figure 3: Measured displacement at the location of the vibrometer. The parametric frequencies indicated on top of the graphs are selected to be close to twice the first natural frequency (10.2Hz). Sweep up (a) and down (b) is shown at different parametric frequencies. (b) At each frequency the data was recorded for 20 seconds. (b) The duration of the tests are varied until the steady-state response was observed.

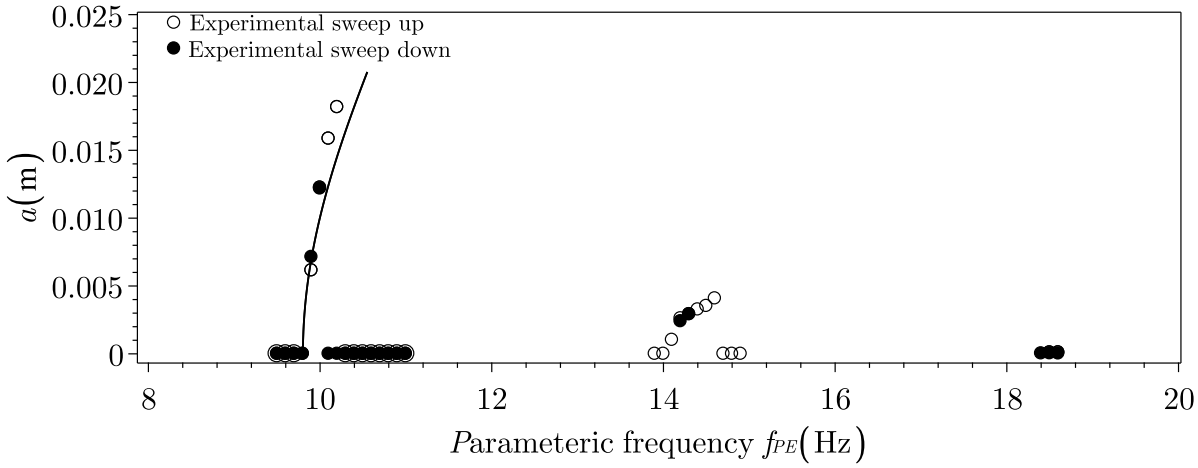

Figure 4: Displacement of the first mass $m_{1\mathrm{m}}$ at different parametric frequencies. Stable solutions are presented analytically for the responses near twice the natural frequency of the first mode. The experimental sweep up and down results show the response at near twice the first natural frequency, combination of the first and the second frequency and twice the second natural frequency.

For the experimental results, Fourier decomposition was employed to extract the solution with a frequency equal to the first resonance.

At the first PR the analytical result Eq. (19) agrees with the experiment (see Fig. 4a). The bifurcation point frequency $f_{\mathrm{branch}} = 4.74\,\mathrm{Hz}$ is predicted correctly by the analytical result. The maximum amplitude at the PR is underestimated by the analytical result. This can be explained most likely by the fact that Eq. (19) is derived by the assumption that $\epsilon_{i,\mathrm{lin}} \ll 1$ while here $\epsilon_{1,\mathrm{lin}} = 127.8$. For PCRs the method presented in [7] is not applicable. Further research is necessary to approximate vibrations at PCRs analytically. At the second PR the bandwidth and the amplitudes are to small to compare analytical and experimental results. Future experiments should aim at tuning the parameters to have a broader bandwidth and higher amplitudes at the second PR in order to compare analytical and experimental results.

6. Conclusion

In this paper, a 2-DOF parametrically excited system was introduced. The experimental set-up and the equation of motion was presented. Steady-state solutions at PR were approximated using analytical approaches and were shown with the experimental results. Comparing the analytical and the experimental results show both the capabilities and the limits of the analytical approximation. The assumption of small parametric excitation $\epsilon_{i,\mathrm{lin}} \ll 1$ for deriving the analytical approximation is heavily violated. Consequently, the vibration amplitudes are underestimated. However, the bifurcation point and hence the bandwidth of the parametric resonance can be predicted correctly. Approximating the vibrations at parametric combination resonances analytically so far is not possible with the method presented. This is a future task to do. A comparison of experimental and analytical results could not be given for the second parametric resonance because of its small bandwidth and small amplitudes. Future experiments should target a broader second PR with higher amplitudes in order to be able to compare the results with the analytical approximation.

References

[1] Huan R, Zhu W, Ma F and Liu Z 2014 The effect of high-frequency parametric excitation on a stochastically driven pantograph-catenary system *Shock and Vibration* **2014**

[2] Larsen J W and Nielsen S R 2007 Nonlinear parametric instability of wind turbine wings *Journal of Sound and Vibration* **299** 64–82

[3] Han Q and Chu F 2013 Parametric instability of a jeffcott rotor with rotationally asymmetric inertia and transverse crack *Nonlinear Dynamics* **73** 827–842

[4] Zaghari B, Ghandchi Tehrani M and Rustighi E 2014 Mechanical modelling of a vibration energy harvester with time-varying stiffness *Proceedings of the 9th International Conference on Structural Dynamics, EURODYN 2014* pp 2079–2085

[5] Dohnal F 2008 Damping by parametric stiffness excitation: resonance and anti-resonance *Journal of Vibration and Control* **14** 669–688

[6] Kniffka T J 2016 *Numerical, semi-analytical and analytical approaches for investigating parametrically excited non-linear systems* Ph.D. thesis Faculty of mechanical and industrial engineering, TU Wien Austria

[7] Kniffka T J, Mace B, Ecker H and Halkyard R 2016 Studies of parametrically excited non-linear mdof systems at parametric resonances *Journal of Physics: Conference Series* vol 744 (IOP Publishing) p 012126

[8] Zaghari B, Rustighi E and Ghandchi Tehrani M 2018 Improved modelling of a nonlinear parametrically excited system with electromagnetic excitation *Vibration* **1** 157–171

[9] Dohnal F 2012 Experimental studies on damping by parametric excitation using electromagnets *Proceedings of the Institution of Mechanical Engineers, Part C: Journal of Mechanical Engineering Science* **226** 2015–2027

[10] Krylov N M and Bogoliubov N N 2016 *Introduction to Non-Linear Mechanics.(AM-11)* vol 11 (Princeton University Press)